European Journal of Mechanics A/Solids 28 (2009) 428–432

Contents lists available at ScienceDirect

European Journal of Mechanics A/Solids

www.elsevier.com/locate/ejmsol

Overspeed burst of elastoviscoplastic rotating disks: Part II – Burst of a superalloy turbine disk

M. Mazière [a,*], J. Besson [a], S. Forest [a], B. Tanguy [a], H. Chalons [b], F. Vogel [b]

[a] MINES ParisTech, MAT–Centre des Matériaux, CNRS UMR 7633, BP 87, 91003 Evry Cedex, France
[b] TURBOMECA F-64511 Bordes, France

ARTICLE INFO

Article history:
Received 9 July 2008
Accepted 6 October 2008
Available online 17 October 2008

Keywords:
Stability
Bifurcation
Non-linear behavior
Rotating disks
Spin-softening
Computational mechanics
Nickel based superalloys

ABSTRACT

Burst of a turbo-engine disk in case of overspeed is investigated both from experimental and computational point of view. Two twin disks made of the same nickel based superalloy are tested. For the first one (B-disk), rotation rate in increased till burst. The second one (S-disk) is kept safe by stopping rotation just before burst, and unloading it to measure residual deformations. The material model parameters are deduced either from simple tension tests, or using an inverse method on the S-disk test. Two corresponding finite element simulations of the B-disk are then performed, using either an arc-length control method to overcome the limit point, or dynamic simulations. In both cases, the numerical burst rotation rate, associated with the loss of stability of the structure, is found to be in good agreement with the experimental result.

1. Introduction

During design of turbo-engines, regulation rules require to demonstrate a significant reserve factor between operating rotation rate and burst rotation rate of critical parts such as disks. Experimental tests are performed on disks in order to validate this reserve factor. Predictions of this experimental bursting speed could be useful to analyze tests and reduce development time. Many methods have been developed for that purpose. First, analytical calculations of deformations in rotating disks have been performed for simple geometries and material behavior. A semi-empirical criterion, based on the calculation of the average hoop stress, has been proposed in Robinson (1944). It is still used to estimate burst speed of disks. But because of complex geometries and material models, this criterion is not precise enough, and numerical finite element simulations are nowadays performed to solve this problem. In the companion paper (Maziere et al., 2008), we have investigated the stability of rotating disks. Two main results were presented in this paper: (I) The overspeed burst rotation rate of a rotating disk can be associated with his loss of stability. This limit rotation rate can be estimated from finite element simulation using either an arc-length control method. In case of a viscoplastic material behavior or dynamic simulations, post-processing tools has been used to estimate the loss of stability of disks. (II) The prediction of the overspeed burst rotation rate highly depends on the characterization of the material behavior. The yield surface and hardening law have to be particularly well described in order to obtain an accurate estimate of this rotation rate.

Analytical solutions of disks with simple geometries are available in Love (1927), Timoshenko and Goodier (1934) for elastic material and in Laszlo (1948) for material with permanent deformations. They provide informations on the stress and strain states in rotating disks. An experimental study of burst strength of disks of uniform thickness is performed in Percy and Ball (1974). Experimental results are compared with analytical solutions and with the semi-empirical criterion proposed by Robinson (1944): a disk will burst when the average hoop stress equals the tensile strength of the material. Still on the same geometry, Tvergaard (1978) performed numerical computations of elastoplastic disks. This latter article focuses on the possibility of bifurcation away from the axisymmetric state, in order to determine if this phenomenon may occur before the maximum rotation rate. All these studies have been performed on axisymmetric disks with simple geometries (rectangle or trapezoidal sections). Actual turbo-engines disks shapes are usually less regular and sometimes non-axisymmetric. Experimental disks used to validate numerical predictions of burst rotation rate are of complex shape with holes and notches. It has been shown in Maziere et al. (2008), Maziere (2006) that empirical criteria are inappropriate to predict the limit load of such disks.

Among turbo-engines, one can make a difference between turbofans (aircraft engines) and turboshafts (helicopter engines). The purpose of a turbofan is to produce thrust by accelerating air through the fan and the engine, while the role of a turboshaft is

* Corresponding author. Tel.: +33 1 60 76 30 45.
E-mail address: maziere@mat.ensmp.fr (M. Mazière).

0997-7538/$ – see front matter
doi:10.1016/j.euromechsol.2008.10.002

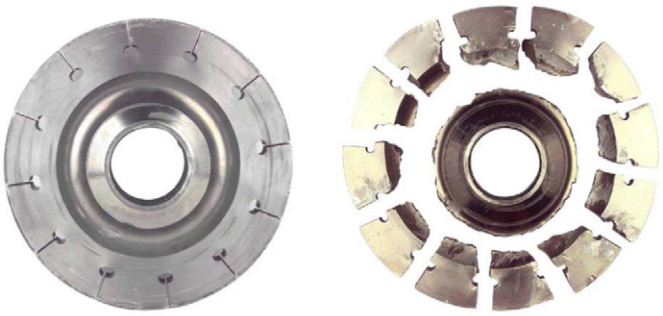

Fig. 1. Photographs of S-disk and B-disk after experiments.

to drive an external rotor. The size and nominal angular velocity of disks also differ. In this paper, an example is given of a test turboshaft disk, which is smaller but rotates faster than turbofan disks. This one is designed in Udimet 720, a nickel based superalloy. Helicopter engines are usually composed of two main turbines. The first one, called "high pressure turbine", is devoted to the production of a flow at a very high speed level from the combustion of high pressure gas. The second one called "power turbine" converts gas flow into rotating power at a very high spin rate.

The aim of this work is to validate the method of prediction based on finite element simulations of the burst rotation rate of elastoplastic experimental disks with complex geometries as proposed in part I (Maziere et al., 2008). For that purpose, two twin experimental disks have been manufactured. The disk denoted B-disk has burst after increasing the rotation rate linearly. The experimental burst rotation rate denoted ω^{EXP} has been measured. The disk denoted S-disk has been stopped at $\omega^{S} = 0.95\omega^{\mathrm{EXP}}$. Inelastic deformations have been measured in order to validate the material behavior. Photographs of the disks after experiments are given in Fig. 1. In this study, finite element simulations are performed on the S-disk in order to validate parameters of the elastoplastic material model. The same model is then used to predict the numerical bursting speed of the B-disk.

Finite element simulations are performed with Zset program (Besson and Foerch, 1997) with a large strain elastoplastic material model presented in Section 2 of part I. Parameters of the model are fitted from simple tensile tests on smooth axisymmetric specimens cut in a third disk. Simple tensile tests on notched axisymmetric specimens (NT) are also performed. Validation of parameters is provided from finite element simulations of notched tensile tests and of the S-disk experiment. Special attention is given to the yield criterion by the introduction of an equivalent stress according to Hosford (1972). Then the numerical burst rotation rate ω^{NUM} of the B-disk is evaluated, using an arc-length control method (Riks, 1979) to overcome the maximal rotation rate. Burst of disk is assumed to coincide with the loss of stability of the structure provided by the global stability condition of (Hill, 1958, 1959; Nguyen, 2000), and then with the maximum of the equilibrium curve. Finally experiments are simulated accounting for inertial terms. Bursts speeds for experiment, static and dynamic simulations are compared for the B-disk.

2. Identification and validation of material parameters

2.1. Identification from smooth tensile specimens

An isotropic elastoplastic model for Udimet 720 at room temperature is proposed in this section. Since deformations of disks are finite, the centrifugal load varies with the rotation rate ω but also with the radius variation of material points. Therefore, finite element simulations have been performed using a finite strain formulation for the material model. Constitutive equations are based on the use of a local objective frame as described in part I (Maziere et al., 2008).

Table 1
Parameters for the nickel based superalloy at 20 °C.

Elasticity		Density		Hardening 1		Hardening 2	
E	200 GPa	ρ	8080 kg m^{-3}	Q_1	2391 MPa	Q_2	−1353 MPa
ν	0.3			b_1	11.1	b_2	17.8
R_0	1211 MPa						

Tensile tests on smooth specimens at different global applied strain rates reveal that yield stress and hardening are: (i) little sensitive to strain rate, (ii) non-linear with two distinct regimes in term of hardening, the stress/strain curve is flat and then hardening. An elastoplastic model is then proposed as follows. The strain rate is split into elastic and plastic contributions. The evolution of the plastic part $\dot{\underset{\sim}{\boldsymbol{e}}}^{p}$ is given by the yield function $f(\underset{\sim}{\boldsymbol{s}}, R)$. The equivalent stress s_{eq} considered is the one proposed in Hosford (1972) and will be discussed further. Finally a non-linear hardening law $R(p)$ is retained with two terms (one for each range of deformation).

$$\dot{\underset{\sim}{\boldsymbol{e}}} = \dot{\underset{\sim}{\boldsymbol{e}}}^{e} + \dot{\underset{\sim}{\boldsymbol{e}}}^{p}, \tag{1}$$

$$f(\underset{\sim}{\boldsymbol{s}}, R) = s_{\mathrm{eq}} - R(p), \tag{2}$$

$$s_{\mathrm{eq}} = \left[\frac{(\sigma_1-\sigma_2)^n + (\sigma_2-\sigma_3)^n + (\sigma_1-\sigma_3)^n}{2}\right]^{1/n} \tag{3}$$

where $\sigma_1 \geqslant \sigma_2 \geqslant \sigma_3$ are the principal stresses and $1 \leqslant n \leqslant \infty$,

$$R(p) = R_0 + Q_1\left(1 - \mathrm{e}^{-b_1 p}\right) + Q_2\left(1 - \mathrm{e}^{-b_2 p}\right), \tag{4}$$

$$\dot{\underset{\sim}{\boldsymbol{e}}}^{p} = \dot{p}\frac{\partial f}{\partial \underset{\sim}{\boldsymbol{s}}}, \quad \dot{p} \geqslant 0, \tag{5}$$

$$\underset{\sim}{\boldsymbol{s}} = 2\mu\underset{\sim}{\boldsymbol{e}}^{e} + \lambda\,\mathrm{tr}(\underset{\sim}{\boldsymbol{e}}^{e})\underset{\sim}{\mathbf{1}}. \tag{6}$$

The Poisson ratio ν and the density of Udimet 720 have been obtained from literature. Other parameters of the model have been identified from a tensile test on a smooth specimen for a global applied strain rate equal to 10^{-3} s^{-1}. Since there is no softening on the conventional stress/strain curve and no necking on tensile specimens (deformations remain homogeneous), the true tensile curve can be plotted easily up to specimen fracture. The Young's modulus E and the yield stress R_0 are identified from the elastic part of the curve, while the hardening law is provided by the plastic range of the curve. The convexity change of curves is made from a combination between an hardening and a softening term in function $R(p)$. Softening parameters, with subscript 2, affect mostly the beginning of the plastic range (up to 5%). Hardening parameters, with subscript 1, affect the whole plastic range. Finally, only the parameter n in the equivalent stress s_{eq} is left undetermined and will be identified below. All other parameters are given in Table 1.

2.2. Identification from notched tensile specimens

Simulations of experiments on smooth and notched tensile specimens have first been performed using the von Mises equivalent stress in the yield criterion. For smooth specimens, the global experimental strain stress curves are obviously accurately reproduced. Indeed, parameters have been calibrated from these curves. However, simulations of notched tensile specimens then overestimate the global stress level (see Fig. 2). Same simulations have then performed with Tresca equivalent stress. Results were found in better agreement with experimental curves even if they lightly underestimate the global stress level. Hosford equivalent stress

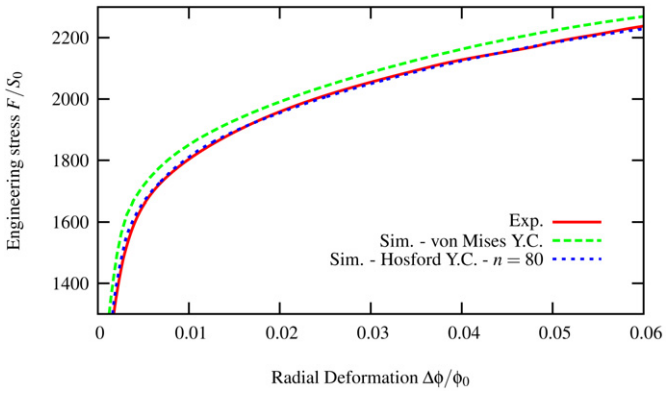

Fig. 2. Experimental equilibrium curve of a notched tensile specimen at 10^{-3} s^{-1}. This deformation rate corresponds to the global axial deformation rate of the notch. Simulations of this equilibrium curve for $n = 4$ (Mises) and $n = 80$.

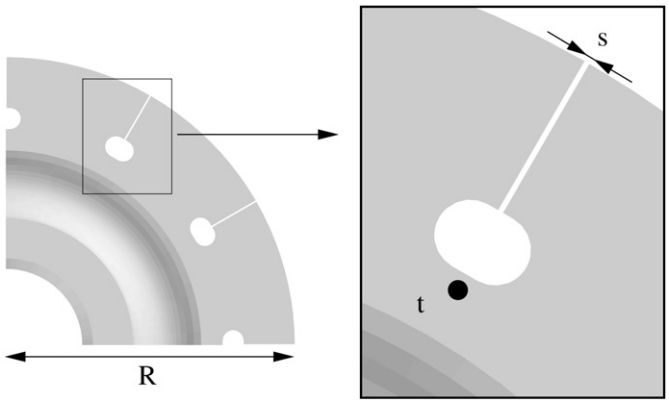

Fig. 3. Location of measured quantities on the S-disk. t denotes the thickness of the disk at the marked point. R is the average radius around the whole disk. s denotes the slot size.

(Hosford, 1972) has finally been chosen to simulate accurately NT experiments.

The parameter n in the equivalent stress definition (see Eq. (6)) allows one to describe either von Mises surface ($n = 2$ or $n = 4$), either Tresca one ($n = 1$ or $n = \infty$), or surfaces between them. The tensile test on smooth specimens cannot be used to identify n because for this particular stress state s_{eq} does not depend on n. An accurate manner to identify n is to perform plane strain or shear tests. The ratio between von Mises and Tresca equivalent stresses for the same strain is then equal to $\sqrt{3}/2$. Indeed, the principal stresses in the local frame for plane strain state are close to $s_1 = s$, $s_2 = s/2$, $s_3 = 0$. Notched tensile specimens are also useful because stress is not homogeneous and covers many points of the yield surface. The resulting average stress is then affected in finite element simulations by the choice of n. Using either elastic (Timoshenko and Goodier, 1934) or elastoplastic (Tvergaard, 1978) behaviors, it can be shown that stress state in a bored disk is close to plane strain state ($\sigma_{rr} \simeq \frac{1}{2}\sigma_{\theta\theta}, \sigma_{zz} \simeq 0$). The knowledge of the actual yield surface is then fundamental for rotating disk simulations. A precise identification of n has been performed using NT tests validated on the S-disk experiment.

The global stress versus radial deformation curve of a notched tensile specimen is plotted in Fig. 2. This experimental result has been compared with finite element simulations of the same specimen using the von Mises equivalent stress ($n = 4$), and an equivalent stress with $n = 80$ (close to Tresca). The latter criterion seems to be more accurate to reproduce experiments. This comparison performed for two geometries of notches (NT2 and NT4), reveals that for the Nickel-based superalloy, Tresca yield criterion is more accurate than von Mises one. $n \simeq 80$ has been identified from these tests.

2.3. Identification from the S-disk

The accuracy of value of n can be validated on the strain prediction from S-disk based by a comparison between experimental residual deformations and numerical ones. Inelastic deformations have been measured on three reference points of the S-disk (see Fig. 3) after interrupting the test before failure. Finite element simulations of the experimental S-disk test have been performed for material models with $n = 4$ (von Mises criterion), $n = 20$, and $n = 80$. The rotation rate has been increased up to ω^S, then the disk was unloaded. Numerical and experimental values of the residual variations of R, t, s are compared in Table 2. Residual deformations $\Delta R/R_0$ and $\Delta t/t_0$ are quite small ($< 5\%$). Then, results given by the three material models are closed. The experimental residual deformation $\Delta s/s_0$ is larger than 100%. Numerical values

Table 2
Experimental and numerical values of residual deformations of reference lengths for $n = 4$ (von Mises yield criterion), $n = 20$, and $n = 80$.

	$\Delta R/R_0$ (%)	$\Delta s/s_0$ (%)	$\Delta t/t_0$ (%)
Experimental	1.2	137	3.3
Mises	0.22	21	0.63
$n = 20$	1	93	2.35
$n = 80$	1.27	119	3.06

are then highly sensitive to material model. This measure is then useful to identify the parameter n. One can observe that results with von Mises criterion and for $n = 20$ underestimate experimental values. The simulation performed with $n = 80$ provides precise estimations of the experimental residual deformation. This model is then retained for the simulation of the B-disk. It must be noted that with $n = 80$, the equivalent stress is very closed to Tresca. However, due to the presence of vertexes on the yield surface, finite element simulation is more difficult with this latter yield criterion. That is why we keep the smooth surface with $n = 80$.

3. Prediction of overspeed burst

3.1. Quasi-static prediction

The simulation of the experimental test on the B-disk is performed on a twenty-fourth of the disk (cf. Fig. 4). The mesh is made of 8 nodes bricks, the selective integration method is used with the finite strain formulation and the elastoplastic law described previously with $n = 80$ (and also with von Mises yield criterion in order to validate the identification of parameter n). The quasi-static computation is performed by prescribing the rotation rate. An arc-length control method is used in order to overcome the limit point induced by geometrical softening. The numerical burst rotation rate ω^{NUM} is then taken at the maximum of the global rotation rate/displacement curve (equilibrium curve). As presented in Maziere et al. (2008), this value coincides with the loss of stability of the structure. This loss of stability coincides with the change of sign of the modified second order work (MSOW) presented in Maziere et al. (2008). The global rotation rate/displacement curve is plotted in Fig. 5 as a function of the normalized radial displacement at the rim of the disk. The rotation rate is normalized with respect to the experimental burst rotation rate ω^{EXP}. One can observe that: (i) the loss of stability of the structure (i.e. when the MSOW become negative) obviously coincides with the limit point of the equilibrium curve (Fig. 6); (ii) using Hosford yield criterion with $n = 80$, the numerical burst rotation rate ω^{NUM} (marked with a $\triangle$) coincides with the experimental one ω^{EXP} with a precision of less than 0.1% showing the

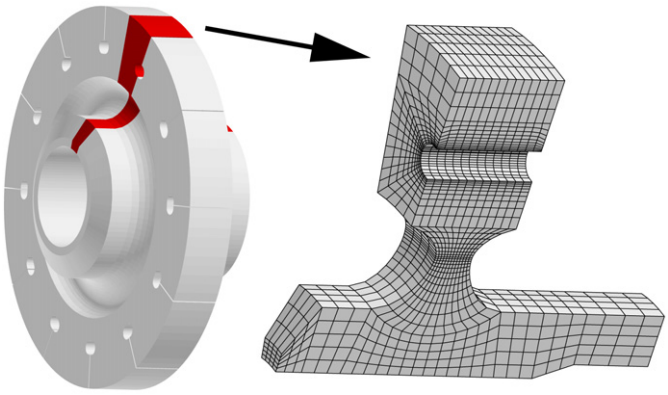

Fig. 4. S-disk and B-disk geometry and mesh.

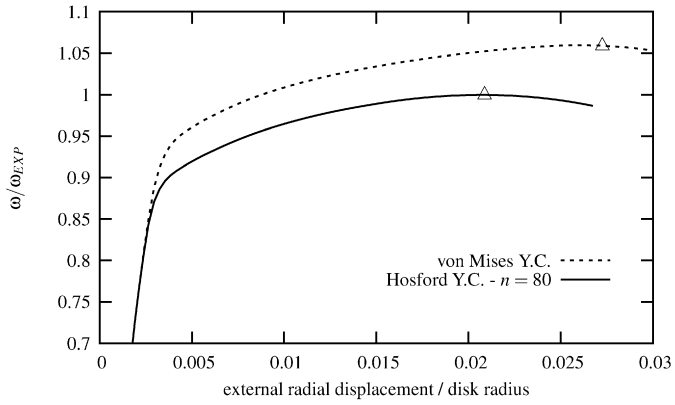

Fig. 5. Simulated equilibrium curve of the B-disk for a static computation. The computed rotation rate is normalized with respect to the experimental burst rotation rate. The equilibrium curve of the same simulation using von Mises equivalent stress overestimates the burst rotation rate.

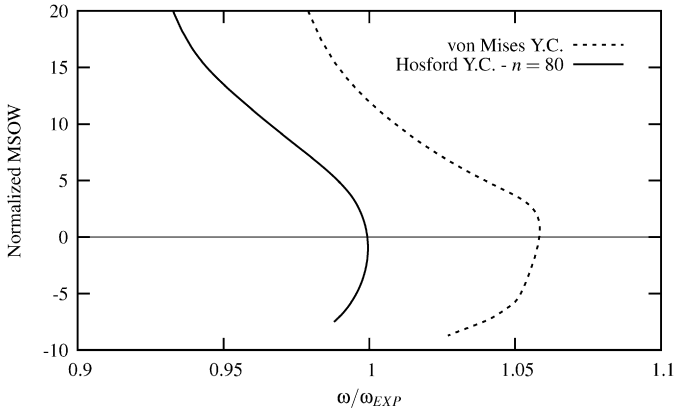

Fig. 6. Modified second order work (MSOW) versus relative rotation rate for simulations of Fig. 5. The MSOW is normalized with respect to the spin-softening term: $\int_{\Omega_0}(\rho_0\|\underline{\boldsymbol{V}}\times\underline{\boldsymbol{\omega}}\|^2)\,dv_0$. When the MSOW is negative or equal to zero, stability is lost.

accuracy of the prediction; (iii) using von Mises yield criterion, the numerical burst rotation rate is more than 5% larger than experimental one.

3.2. Dynamic prediction

The simulation performed in the previous part is accurate to predict the experimental burst rotation rate, but the post-critical behavior is not correctly described using the arc-length control method. Indeed, during experiment, the rotation rate increases linearly up to burst which occurs suddenly. The "loading" path is such that the rotation rate increases from 0 rpm up to ω^{EXP} in almost 300 s. The rotation rate does not decrease like in the quasi-static simulation performed with the arc-length method. An alternative method to reliably reproduce the experiment is to perform simulations taking the dynamic term in the equilibrium equation into account (Maziere et al., 2008). The arc-length control method is not needed anymore. The simulation is performed with the same implicit finite element program as previously. As remarked by Bathe (1996), the inertial effect of the dynamic case is useful to assure convergence in strongly non-linear problems even when there is effectively no global dynamic effect.

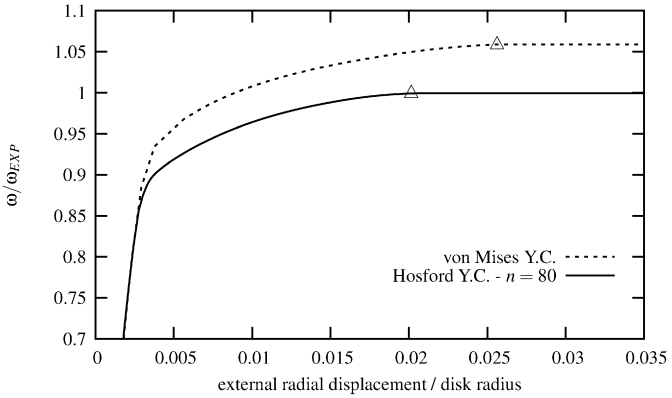

Fig. 7. Simulated equilibrium curve of the B-disk for a dynamic computation. The computed rotation rate is normalized with respect to the experimental burst rotation rate.

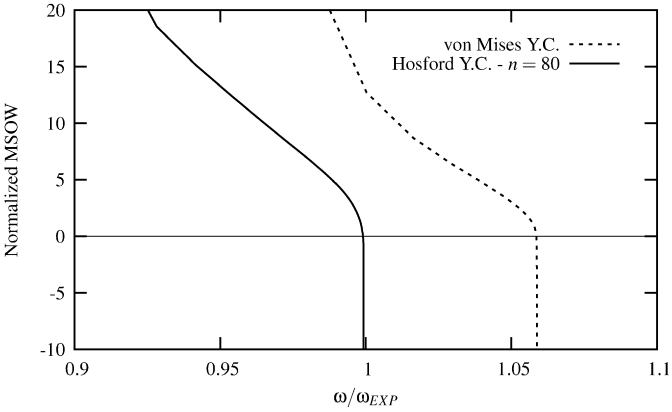

Fig. 8. Modified second order work (MSOW) versus relative rotation rate for simulations of figure 7. The MSOW is normalized with respect to the spin-softening term: $\int_{\Omega_0}(\rho_0\|\underline{\boldsymbol{V}}\times\underline{\boldsymbol{\omega}}\|^2)\,dv_0$. When the MSOW is negative or equal to zero, stability is lost.

The limit point (marked with a △) is defined from the stability condition as presented in Fig. 7. The experimental burst rotation rate is again accurately predicted using Hosford yield criterion with $n = 80$, and overestimated using von Mises one (Fig. 8). The local acceleration remains almost null while the rotation rate increases significantly. The dynamic computation coincides with the static one, until the rotation rate reaches the maximum of the equilibrium curve, the MSOW becomes negative and the accelerations of displacements increase roughly (see Fig. 9) to keep the rotation rate nearly constant. Deformations dramatically increase in some zones of the structure where the fracture of the disk should occur.

4. Conclusion

In order to validate the method presented in Maziere et al. (2008) to predict the burst rotation rate of rotating disks in case

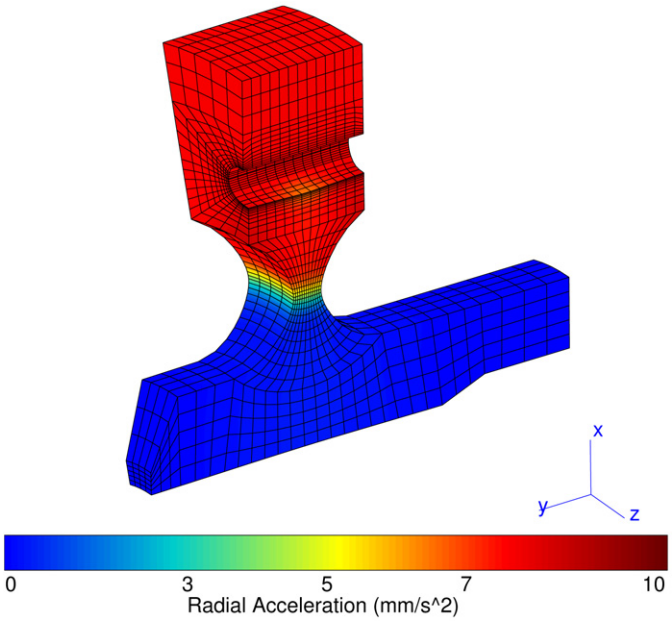

Fig. 9. Radial acceleration at the instability point (△) for the simulation using Hosford yield criterion with $n = 80$.

of overspeed, some experiments were performed on tensile specimens and on experimental disks. The material behavior has been identified: (I) On smooth tensile specimens for almost all elasto-plastic parameters; (II) On notched tensile specimens for the parameter n of the original Hosford yield criterion. Then two experimental disks were tested: (III) The S-disk was loaded and unloaded just before burst in oder to validate the parameter n. (IV) The B-disk was loaded up to burst. Its burst rotation rate was accurately predicted either from a quasi-static finite-element simulation using an arc-length control method, and from a dynamic one using Hill stability criterion to detect the limit rotation rate.

A strong sensitivity of the burst rotation rate and of the local plastic strain has been found with respect to the choice of the yield function. For the investigated material, a close to Tresca criterion turns out to be more reliable than von Mises. Other origins may exist to explain discrepancy between experiment burst rate and numerical prediction: local anisotropy induced by forging, residual stress, temperature dependence of material behavior.... The computational tools developed in this work can be used in future work to analyze the effect of these material characteristics.

Acknowledgements

This work has been carried within the common project DDV leaded by ONERA (French Aeronautics and Space Research Center) and funded by the DGA (French Ministry of Defense) which is gratefully acknowledged.

References

Bathe, K., 1996. Finite Element Procedure. Prentice-Hall.
Besson, J., Foerch, R., 1997. Large scale object-oriented finite element code design. Comput. Methods Appl. Mech. Engrg. 142, 165–187.
Hill, R., 1958. A general theory of uniqueness and stability in elastic-plastic solids. J. Mech. Phys. Solids 6, 236–249.
Hill, R., 1959. Some basic principles in the mechanics of solids without a natural time. J. Mech. Phys. Solids 7, 209–225.
Hosford, W., 1972. A generalized isotropic yield criterion. J. Appl. Mech. 39, 607–609.
Laszlo, F. 1948. Rotating disks in the region of permanent deformation. Technical report, National Advisory Committee for Aeronautics.
Love, A., 1927. A Treatise on the Mathematical Theory of Elasticty. Dover Edition.
Maziere, M., 2006. Overspeed burst of turboengine disks. PhD thesis, Mines Paris–ParisTech.
Maziere, M., Besson, J., Forest, S., Tanguy, B., Chalons, H., Vogel, F., 2008. Overspeed burst of elastoviscoplastic rotating disks – Part I: Analytical and numerical stability analyses. Eur. J. Mech., doi:10.1016/j.euromechsol.2008.07.008.
Nguyen, Q., 2000. Stability and Nonlinear Solid Mechanics. John Wiley & Sons.
Percy, M., Ball, K., Mellor, P., 1974. An experimental study of the burst strength of rotating disks. Int. J. Mech. Sci. 16, 809–817.
Riks, E., 1979. An incremental approach to the solution of snapping and buckling problems. Int. J. Solids Structures 15, 529–551.
Robinson, E., 1944. Bursting tests of steam-turbine disk wheels. Trans. ASME 66, 373.
Timoshenko, S., Goodier, J., 1934. Theory of Elasticity. McGraw-Hill Edition.
Tvergaard, V., 1978. On the burst strength and necking behavior of rotating disks. Int. J. Mech. Sci. 20, 109–120.